



# **Performance Analysis of SMQW SOA Based On Optical Confinement Factor**

Nipu R. Barai<sup>1</sup>, Rinku Basak<sup>2</sup>

M.Sc. Student, Dept. of Electrical and Electronic Engineering, American International University-Bangladesh, Dhaka,  
Bangladesh<sup>1</sup>

Assistant Professor and Head of Graduate Program, Faculty of Engineering, American International University-  
Bangladesh, Dhaka, Bangladesh<sup>2</sup>

**ABSTRACT:** Study of the dependency of optical confinement factor (OCF) on the structure parameters of symmetrical multiple quantum well (SMQW) semiconductor optical amplifier (SOA) is important for better design of SOA devices. This paper presents an overall structure of a SMQW SOA, and dependency analysis of OCF on different structure parameters. The effects of number of well layers, well thickness and barrier thickness of SMQW SOA on OCF are investigated through simulations performed using MATLAB. The simulation results show that OCF of a SMQW SOA increases with increasing number of quantum well layers and well layer thickness. However, the change in barrier thickness doesn't have significant impact on the OCF. The simulation results also indicate that with appropriate number of well layers and well layer thickness, it is possible to obtain a better OCF. The findings of this study can be used for creating more efficient and stable SMQW SOA design.

**KEYWORDS:** Symmetrical Multiple Quantum-well, Semiconductor Optical Amplifier, Optical Confinement Factor.

## **I. INTRODUCTION**

Semiconductor optical amplifier, referred to as SOA, is used for many applications in all-optical systems including amplification of the optical signal without converting it into electrical signal [1]. SOA is becoming popular because it is suitable for integration and it can be used as functional devices. In addition, it can operate in a wide bandwidth region. There are many types of SOA depending on the construction of its active region (e.g., multiple quantum well (MQW) SOA, travelling wave (TW) SOA, quantum dot (QW) SOA, gain clamped (GC) SOA) [2-3]. Based on the quantum well layers MQW SOA can be divided into two types, the symmetrical MQW SOA and the asymmetrical MQW SOA. Symmetrical multiple quantum well (SMQW) SOA is the focus point of this paper. The structure of SMQW SOA is similar to that of a semiconductor laser. The main difference is in the anti-reflective mirror (or coating) on both of its facets [4]. The fabrication of the active region is done by loading well and barrier layers. These layers are grown using different types of growth technique such as molecular beam epitaxy (MBE), organo-metallic vapour epitaxy (OMVPE) [2]. The advantages of using SMQW SOA are its ability to perform at original to ultra-long wavelength band, higher saturation output, ultrafast gain recovery, low noise operation, control polarization sensitivity, compactness, and cost-effectiveness [5-7]. Some of the drawbacks include narrower full width half maximum (FWHM) gain bandwidth and complexity in growing layers [8-9].

For performance analysis and comparison with other types of SOAs, a clear understanding of the dependency on various factors is necessary for SMQW SOA. One of these factors is the optical confinement factor (OCF). The dependency of OCF on the number of layers and layer thicknesses is important for the performance analysis of the device. The performance analysis is also important for designing both the SMQW SOA and an SMQW SOA, and for the comparison of their performances. In addition, the analysis of the dependency of saturation power on the structure parameters is also useful. Therefore, the main objective of this work is to analyse the dependencies of OCF on SMQW SOA structure parameters by performing computer simulations.

**II. THEORETICAL BACKGROUND**

A simplified schematic structure of 3D SMQW SOA is shown in Fig. 1. It shows the wells and barrier layers of the active region, as well as the cladding layers. In this case, it is considered that the active region length is equal to the cavity length, and the taper length,  $L_t$ , is equal to zero. The length of the active region ( $L$ ) is given by [11],

$$L = L_c \tag{1}$$

where,  $L_c$  is the cavity length. The amplifier is designed with negligible facet reflectivity to ensure a single pass.

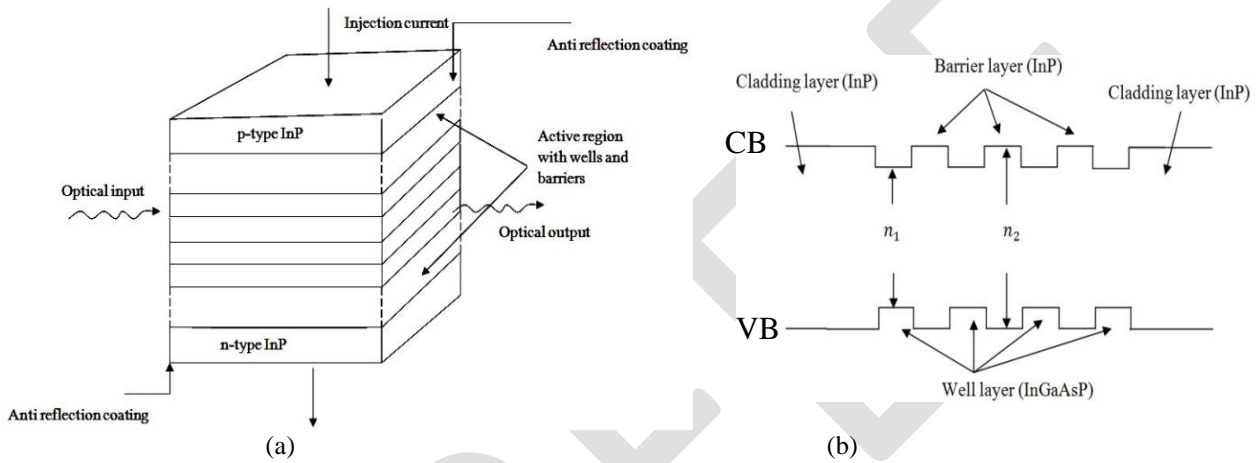


**Fig. 1.** Schematic diagram of (a) Basic SMQW SOA (3D view).

Injection current direction and power direction is shown. Length of the active region is considered to be equal to the length of the cavity region and the taper length is ignored. The active region is sandwiched between the two doped cladding layers and the number of wells and barrier layers can be varied according to the need of the application. (b) Basic structure of the conduction band (CB) and valence band (VB) of a SMQW SOA where the cladding and barrier material is InP and the well material is InGaAsP. Here  $n_1$  and  $n_2$  are refractive indices of the well and barrier layers and ( $n_1 > n_2$ ).

The injection current ( $I$ ) is related to the carrier density ( $n$ ) by [12],

$$I = \frac{qVn}{\tau_c} \tag{2}$$

where,  $q$  is the electron charge,  $V$  is the volume of the active region,  $n$  is the carrier density and  $\tau_c$  is the carrier lifetime. Carrier lifetime is non linearly dependent to the Auger nonradiative recombination in InGaAsP material system as [13],

$$\tau_c = \frac{1}{A_{nr} + Bn + Cn^2} \tag{3}$$

where,  $A_{nr}$  is nonradiative recombination coefficient,  $B$  is the bimolecular radiative recombination coefficient and  $C$  is the Auger non radiative recombination coefficient.

The saturation power dependency on the material parameters can be expressed as [12],

$$P_{sat} = (hc_0 wd) / (\lambda_0 \Gamma a) [A_{nr} + B \left( n_0 + \frac{\alpha + (\ln G_s \Gamma)}{\Gamma a} \right) + C \left( n_0 + \frac{\alpha + (\ln G_s \Gamma)}{\Gamma a} \right)^2] \tag{4}$$



# International Journal of Advanced Research in Electrical, Electronics and Instrumentation Engineering

(An ISO 3297: 2007 Certified Organization)

Vol. 3, Issue 8, August 2014

$$n = n_0 + \frac{\alpha + (\ln G_s / \Gamma)}{\Gamma a} \quad (5)$$

$$G_s = \exp[\Gamma(g_s - \alpha)L] \quad (6)$$

where,  $n$  is the carrier density,  $n_0$  is the carrier density for transparency,  $\Gamma$  is the optical confinement factor,  $\alpha$  is the insertion loss,  $a$  is the material gain co-efficient,  $h$  is the Planck's constant,  $c_0$  is the speed of light in vacuum and  $\lambda_0$  is 1.55  $\mu\text{m}$ . OCF is related to the active layer parameters and refractive indices of the layer materials [2].

$$\Gamma = \frac{\gamma N_w d_w}{(N_w d_w + N_b d_b)} \quad (7)$$

where, co-efficient  $\gamma$  is related to the effective refractive index by,

$$\gamma = 2\pi^2 (N_w d_w + N_b d_b)^2 \left( \frac{\mu_{\text{eff}}^2 - \mu_c^2}{\lambda_0^2} \right) \quad (8)$$

where,  $\mu_{\text{eff}}$  is the effective refractive index. This is also related to the refractive indices and the layer parameters by [12],

$$\mu_{\text{eff}} = \frac{(N_w d_w \mu_w + N_b d_b \mu_b)}{(N_w d_w + N_b d_b)} \quad (9)$$

where,  $N_w$  is the number of wells,  $N_b$  is the number of barriers denoted by  $(N_w - 1)$ ,  $d_w$  is the well thickness,  $d_b$  is the barrier thickness,  $\mu_w$  is the refractive index of the well layer material (InGaAsP in this case),  $\mu_b$  is the refractive index of the barrier material ( here, InP). Substitution of the value of equation (9) into equation (8) provides,

$$\gamma = 2\pi^2 (N_w d_w + N_b d_b)^2 \left( \frac{(N_w d_w \mu_w + N_b d_b \mu_b)^2 - \mu_c^2}{\lambda_0^2} \right) \quad (10)$$

Now, for SMQW SOA the relation of optical confinement factor with the structure parameters can be expressed as,

$$\Gamma = \frac{2\pi^2 (N_w d_w + N_b d_b)^2 \left( \frac{(N_w d_w \mu_w + N_b d_b \mu_b)^2}{\lambda_0^2} - \mu_b^2 \right) N_w d_w}{(N_w d_w + N_b d_b)} \quad (11)$$

For single QW, the optical confinement factor is expressed as,

$$\Gamma_{\text{sqw}} = \frac{2\pi^2 N_w^2 N_b^2 (\mu_{\text{eff}}^2 - \mu_b^2)}{\lambda_0^2} \quad (12)$$

OCF is the ratio of light intensity within the active region to the total light intensity. It is defined as 'Γ'. As the name indicates, the light is needed to be confined in the active region for the operation and not being scattered or absorbed by other layers. Therefore, a higher OCF is required. Usually in laser operation the value of OCF is kept 0.4 or more for a stable operation. In SMQW SOA, OCF of 0.3 to 0.6 is acceptable for better performance. In large modulation bandwidth systems, higher OCF is required [15-16]. OCF depends on the molar fraction and thus related to the material composition [2] which leads to the quantum well and material well materials.

### III.SIMULATIONS

The equations explained in the previous section for SMQW SOA were used to perform various simulations. The computer codes for these equations were generated in MATLAB 7.10.0. The device can be observed using OptiSystem software, if needed. For the simulations presented in this paper, taper length is omitted to avoid complexity of the calculations. The compounds chosen for this study are quite popular for experiments now-a-days. It is 1.55  $\mu\text{m}$



# International Journal of Advanced Research in Electrical, Electronics and Instrumentation Engineering

(An ISO 3297: 2007 Certified Organization)

Vol. 3, Issue 8, August 2014

InP/InGaAsP system. The most important criteria for selection of well layers and barrier layers are that the band-gap energy of the well layer (InGaAsP) is lower than the band-gap energy of the barrier layer (InP), and the refractive index is greater for the well material. The lattice parameters are also required to be matched (5.8694 Å in this case) [10]. The composition of the compounds expressed in the form of  $\text{In}_{1-x}\text{Ga}_x\text{As}_y\text{P}_{1-y}$  [10]. Compositions including the molar fraction values are not provided in details here. The values of various parameters in the simulations are provided in Table 1 [14].

TABLE I  
SMQW SOA STRUCTURE AND MATERIAL PARAMETERS

Symbol	Parameter	Value
$\lambda_0$	Operating wavelength	1.55 $\mu\text{m}$
$L$	Length of the active region	500 $\mu\text{m}$
$w$	Width of the active region	1 $\mu\text{m}$
$d_w$	Thickness of the well layer	0.01 $\mu\text{m}$
$d_b$	Thickness of the barrier layer	0.01 $\mu\text{m}$
$\mu_w$	Refractive index of the well layer material	3.54
$\mu_b$	Refractive index of the barrier layer material	3.18
$\mu_c$	Refractive index of the cladding layer material	3.18
$A_{nr}$	Non-radiative recombination coefficient	1e9 /s
$B$	Bimolecular radiative recombination coefficient	1e-10 $\text{cm}^3/\text{s}$
$C$	Auger non radiative recombination coefficient	3x1e-29 $\text{cm}^6/\text{s}$
$G_s$	Small signal material gain	30 dB

## IV. RESULTS AND DISCUSSION

The change in OCF is observed for variation of different structure parameters, e.g., number of quantum wells, number of barriers, well layer thickness and barrier layer thickness. Fig. shows the change in OCF due to the variation of the number of well layers between 0 and 20. The results indicate that with the increase in number of well layers, OCF is increased exponentially with the values between 0 and 0.8. Fig. 2 presents the dependency of OCF on increasing number of wells in the active region. For lower number of wells the OCF has a lower value. When the complexity of the growing layers is avoided, and there are limitations in choosing higher number of wells, the SMQW SOA can be designed with lower number of well layers. However, the tradeoff would be lower OCF.

The change of OCF due to the change in the number of barrier layers is shown in Fig. 3. The number of barriers ( $N_b$ ) is equal to ( $N_w-1$ ); therefore, the trend of OCF versus number of barriers curve (Fig. 3) is similar to that OCF versus number of wells curve (Fig. 2). When the number of barriers is varied from 3 to 12 (with the number of wells varied from 4 to 13), the OCF changes from 0 to 0.35.

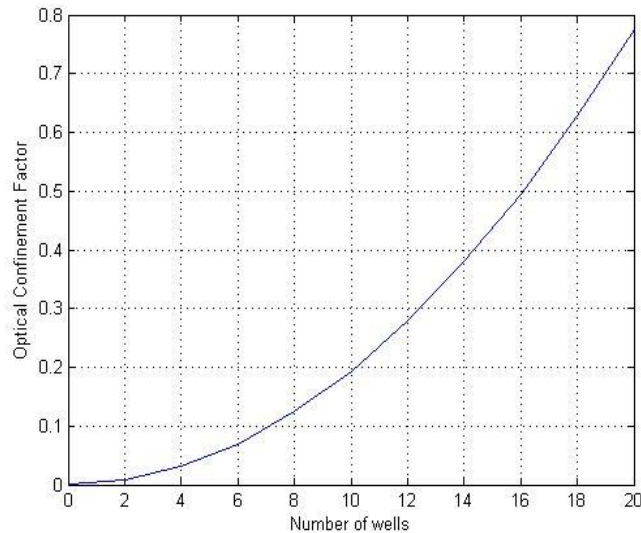


**Fig. 2.** Variation of OCF with the increasing number of wells. When the number of wells are varied from 0 to 20, the OCF is increased exponentially from 0 to 0.8.

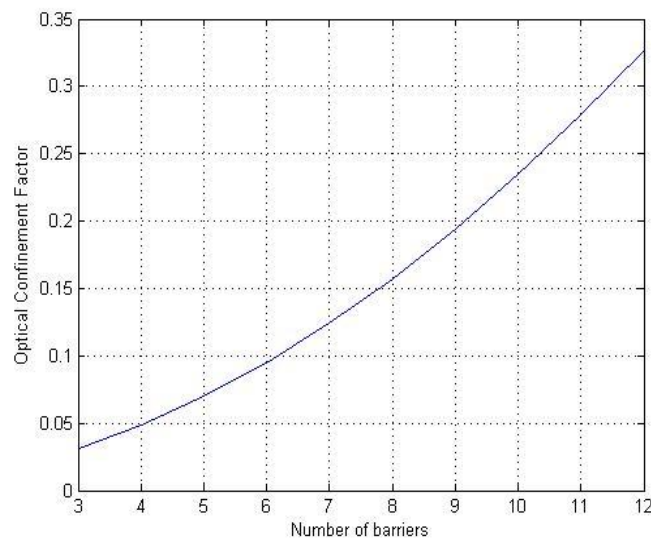


**Fig. 3.** Variation of OCF with the increasing number of barrier layers. For  $N_w$  wells the number of barrier is  $(N_w - 1)$ .

The change in OCF is obtained through simulations by varying the well layer thickness for 4, 10, 15 number of well layers. Fig.4 shows the OCF versus well thickness curve for 4 wellled active region SMQW SOA. When the number of barriers is 3, the OCF varies from approximately 0.005 to 0.06 for the well thickness variation from 4nm to 13nm. The range of OCF here is low.

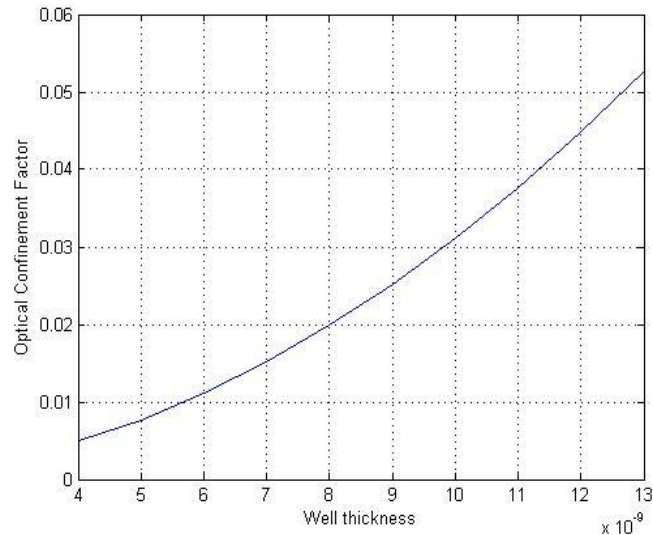


**Fig. 4.** Variation of OCF with the increasing well thickness in the active region for 4 QWs.

For the well thickness range of 4 nm to 13 nm, 10 and 15 well layered devices are also analyzed. Fig. 5 shows the OCF versus well thickness curve for 10 well layered active region SMQW SOA. When the number of barriers is 9, the OCF varies from approximately 0.03 to 0.35 for the well thickness variation from 4nm to 13nm. The range of OCF here is higher than the previous case.

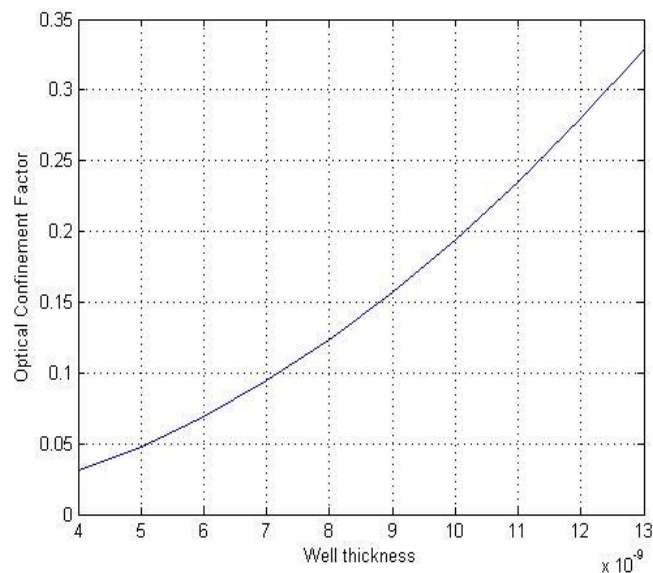


**Fig. 5.** Variation of OCF with the increasing well thickness in the active region for 10 QWs.

Fig. 6 shows the OCF versus well thickness curve for 15 well layered active region SMQW SOA. When the number of barriers is 14, the OCF varies from approximately 0.085 to 0.8 for the well thickness variation from 4nm to 13nm. The range of OCF here is higher than both 4 and 10 quantum well active region.

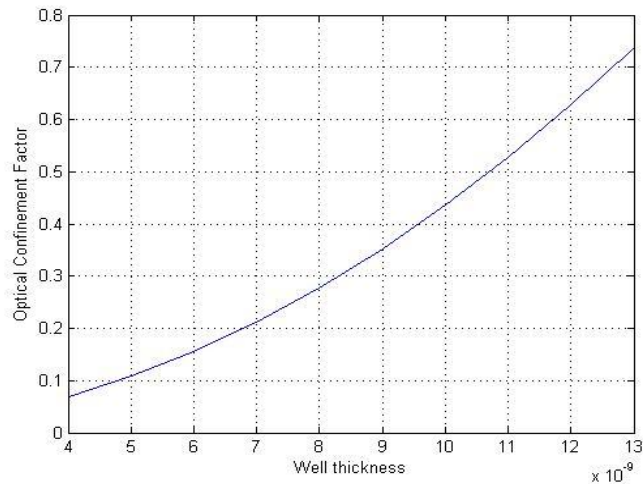


**Fig. 6.** Variation of OCF with the increasing well thickness in the active region for 15 QWs.

The results shown in Fig. 4, Fig. 5 and Fig. 6 indicate that for the same thickness range (4 nm to 13 nm), SMQW SOA designed with 10 to 15 quantum wells shows higher OCF.

In order to observe the change in OCF for different barrier layer thicknesses, the barrier thickness is varied from 4 nm to 13 nm. The OCF versus barrier thickness graph is determined for both 4 wells and 10 wells. In both of the cases, the OCF shows minor decrement with the increasing barrier thickness. From Fig. 7 it can be established that the OCF does not depend on barrier thickness (for 10 wells). The increase in barrier thickness from 4 nm to 13 nm results in the OCF changes from 0.193 to 0.1965.

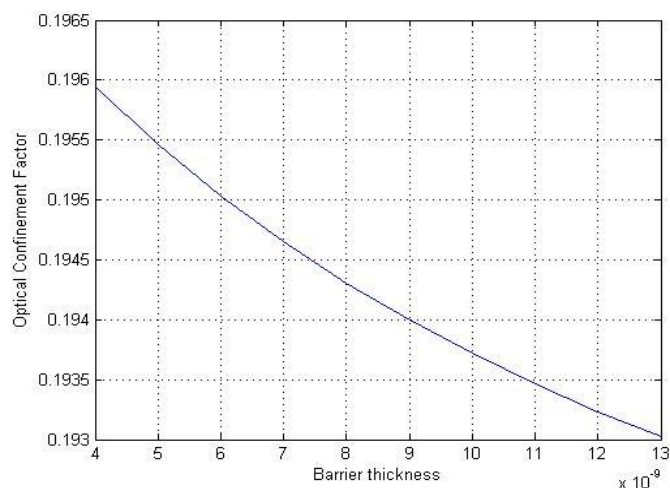


**Fig. 7.** Variation of OCF with the increasing barrier thickness in the active region for 10 QWs.

### V.CONCLUSION

The simulations and dependency analysis results show that the OCF is highly sensitive to the change in well thickness and number of well layers, and less sensitive to the change in barrier thickness. The target for a device structure is to use the design parameters that lead to better OCF. Analysis of the various graphs indicates that when the number of well layers in a SMQW SOA is varied from 10 to 15 with 10 nm to 13 nm of well layer thickness, it would be possible to obtain a better OCF. High OCF leads to higher stability of the device. It affects the modal condition (TE or TM, single



# International Journal of Advanced Research in Electrical, Electronics and Instrumentation Engineering

(An ISO 3297: 2007 Certified Organization)

Vol. 3, Issue 8, August 2014

or multiple modes), divergence as well as the threshold current conditions [17]. Therefore, OCF is very important while designing a SMQW SOA. A major drawback of using SOA is the pattern effect; however, solutions are available such as using Lyot filter [18].

## REFERENCES

- [1] M. J. Connelly, "Semiconductor optical amplifiers", Dordrecht, the Netherlands: Kluwer Academic Publishers, ch.1-3, pp.1-41, 2002.
- [2] N. K. Dutta, Q. Wang, "Semiconductor optical amplifiers", 5 Toh Tuck Link, Singapore: World Scientific Publishing Co. Pte. Ltd, ch.1-2, 2006.
- [3] J. Bernard and M. Renaud, "Semiconductor Optical Amplifiers", SPIE's OE Magazine, Vol.1, No.1, pp. 36-38, Sep. 2001.
- [4] T. Durhuus, B. Mikkelsen, K. E. Stubkjaer, "Detailed Dynamic model for semiconductor optical amplifiers and their crosstalk and intermodulation distortion", Journal of Lightwave Technology, Vol.10, pp.1056-1064, 1992.
- [5] T. Motaweh, P. Morel, A. Sharaiha, M. Guegan, "A Semi-phenomenological model for the material gain of broadband MQW-SOAs", 13<sup>th</sup> conference of Numerical Simulation of Optoelectronic devices (NUSOD), pp. 43-44, 19-22, 2013.
- [6] M. Babaei, S. S. Hosseini, and S. M. Kuchaki, "Improving gain and saturation output power in single-quantum-well semiconductor optical amplifiers", IEEE Journal of Quantum Electronics, Vol.45, pp.342-347, 2010.
- [7] H. J. S. Dorren, X. Yang, D. Lenstra, H. de Waardt, G. D. Khoe, T. Simyama, H. Ishikawa, H. Kawashima, and T. Hasama, "Ultrafast refractive index dynamics in a multiple quantum well semiconductor optical amplifier", IEEE Photonics tech. letters, Vol.15, No.6, 2003.
- [8] V. V. Lysak, H. Kawaguchi, and I. A. Sukhoivanov, "Gain spectra and saturation power of asymmetrical multiple quantum well semiconductor optical amplifiers", IEE Proc.-Optoelectronic., Vol.152, No.2, 2005.
- [9] W. Loh, J. J. Plant, J. Klamkin, J. P. Donnelly, F. J. Odonnell, R. J. Ram, P. W. Juodawlkis, "Limitations of noise figure in InGaAsP quantum well semiconductor optical amplifiers", CLEO and QELS Conference, San Jose, CA, pp.1-2, 2010.
- [10] G. H. Olsen, T. Z. Zamerowski, R. T. Smith, E. P. Bertin, "InGaAsP quaternary alloys: composition, refractive index and lattice mismatch", Journal of Electronic Materials, Vol.9, No.6, 1980.
- [11] M. J. Connelly, "Wideband Semiconductor Optical Amplifier Steady-State Numerical Model", IEEE Journal of Quantum Electronics, Vol.37, No.3, 2001.
- [12] A. A. Al-mfiji, "Saturation Gain Characteristics of Quantum-Well Semiconductor Optical Amplifier". Nahrain University, College of Engineering J. (NUCEJ), Vol.14, No.2, pp.205-212, 2011.
- [13] F. Wang, G. Xia, and Z. Wu, "Numerical study of mode-locked semiconductor optical amplifier fiber ring laser", J. Optoelectronics and Advanced Materials, Vol.8, No.3, pp.1267-1272, 2006.
- [14] A. A. Lobintsov, M. B. Uspenskii, V. A. Shishkin, M. V. Shramenko, and S. D. Yakubovich, "Highly efficient semiconductor optical amplifier for 820-860 nm spectral range", IEEE J. Quantum Electronics, Vol.40, No.4, 2010.
- [15] J. Shimizu, H. Yamada, S. Murata, A. Tomita, M. Kitamura, and A. Suzuki, "Optical Confinement Factor Dependencies of the K factor, Differential Gain, and Nonlinear Gain Coefficient for 1.55um InGaAs/InGaAsP MQW and Strained-MQW Lasers", IEEE Photonics technology letter, Vol.3, No.9, 1991.
- [16] Y. Z. Huang, Z. Pan, and R. H. Wu, "Analysis of the optical confinement factor in semiconductor lasers", Journal of Applied Physics, Vol.79, No.8, 1996.
- [17] T. D. Visser, H. Blok, B. Demeulenaere, and D. Lenstra, "Confinement factors and gain in optical amplifiers", IEEE Journal of Quantum Electronics, Vol.33, No.10, 1997.
- [18] Z. V. Rizou, K. E. Zoiros, A. Hatziefremidis, M. J. Connelly, "Design Analysis and Performance Optimization of a Lyot Filter for Semiconductor Optical Amplifier Pattern Effect Suppression", IEEE Journal of selected topics in quantum electronics, Vol.19, No.5, 2013.